Electronic Supporting Information

Tungsten Oxide-Coated Copper Gallium Selenide Sustains Long-Term Solar Hydrogen Evolution

David W. Palm,[†] Christopher P. Muzzillo,[‡] Micha Ben-Naim,[†] Imran Khan,[‡] Nicolas Gaillard,[§] Thomas F. Jaramillo[†‖]

[†]Department of Chemical Engineering, Stanford University, 443 Via Ortega, Stanford, California 94305, United States

[‡]National Renewable Energy Laboratory, 15013 Denver W Pkwy, Golden, Colorado 80401, United States

[§]Hawaii Natural Energy Institute (HNEI), University of Hawaii, 1680 East−West Rd POST 109, Honolulu, Hawaii 96822, United States

[‖]SUNCAT Center for Interface Science and Catalysis, SLAC National Accelerator Laboratory, 2575 Sand Hill Road, Menlo Park, California 94025, United States

Methodology

Materials

Bis(*tert*-butylimino)bis(dimethylamino)tungsten(VI) (BTBMW, 97%) was purchased from Strem Chemicals, sulfuric acid (H_2SO_4, 99.999%) was purchased from Sigma-Aldrich, and perchloric acid ($HClO_4$, 70% Veritas double distilled) was purchased from GFS Chemicals. Deionized water (DI H_2O, 18.2 MΩ·cm) from a Millipore Q-POD® system was used to dilute the concentrated acids to the appropriate electrolyte concentrations. The hydrogen evolution reaction (HER) catalyst analogue electrodes were prepared from degenerately-doped n-type silicon (n^+Si) wafers (<100> surface facet, .001-.005 Ω-cm, single-side polished, prime grade, 500-550 μm) from Nova Electronic Materials.

Materials Characterization

Spectroscopic ellipsometry was performed using a Woollam M-2000® ellipsometer, where the coated silicon wafer substrate was characterized over the incidence angles of 65-75°. The data were fit to built-in models on the WVASE® analysis software in order to determine the thickness of the deposited WO_3 film. Scanning electron micrographs and EDX spectra and elemental maps were obtained using an FEI Magellan 400 XHR Scanning Electron Microscope equipped with a Thermo Fisher Scientific Pathfinder EDS UltraDry 60 M with Pinnacle software. The measurements were obtained with a beam voltage and current of 3 kV and 3.2 nA, respectively, chosen to optimize signal from the ultrathin films under investigation in this study. An Agilent Cary 6000i UV/Vis/NIR spectrophotometer was used in transmittance mode to interrogate the optical properties of the ultrathin protective and catalytic coatings. The coatings were coated onto transparent quartz substrates and the measurements were baseline-corrected for these quartz substrates. Grazing incidence x-ray diffraction (GI-XRD) measurements were performed on a Bruker D8 Venture instrument utilizing a Cu anode (8.04 keV) and a two-dimensional PHOTON 100 detector, with incidence angles ranging from 1° to 5° and a collection time of 60 s.

Synthesis

For the synthesis of $CuGa_3Se_5$ absorbers, soda-lime glass was first coated with a Mo back contact (800 nm; direct-current sputtered). Three-stage co-evaporation (metal and Se, simultaneously) was then performed: Ga was first evaporated at 4.4 Å/s onto the substrate held at 400 °C with a Se/Ga molar flux of 9. Second, Cu was evaporated at 3.5 Å/s at a substrate temperature of 600 °C and Se/Cu of 7 until the film became Cu-rich (Cu/Ga > 1, as evidenced by a ~1 °C substrate temperature dip associated with a change in emissivity). In the third stage, Ga and Se evaporation was resumed as in stage 1 while the substrate was held at 600 °C. The final $CuGa_3Se_5$ films were 2.5 μm thick (by Dektak 8 profilometer) and had Cu/Ga compositions of 0.33 to 0.36 (by X-ray fluorescence).

Pulsed chemical vapor deposition of the ultrathin WO_3 coatings was performed in a Fiji F202 system from Cambridge Nanotech. The BTBMW precursor was preheated to 95 °C and DI H_2O was used as the oxidizing agent. The reactor and substrate plate temperatures were held at 300 °C and 350 °C, respectively, throughout the deposition. The BTBMW and DI H_2O were pulsed in alternating fashion for 2 s and 0.1 s, respectively, with 20 s of argon gas purging in between for a total of 600 cycles. The WO_3 film thickness of 3.8 nm was utilized in this study because this synthetic route appeared to exhibit a self-limiting behavior, where depositing more film became increasingly challenging beyond this thickness. This synthetic challenge means that the thickness of the WO_3 coating is not necessarily optimal, an opportunity for further studies.

A platinum nanoparticulate coating was deposited in an electron beam evaporation system from AJA International using a Pt metal source at a rate of 0.05 nm s^{-1} to a nominal thickness of 1 nm, as measured by a quartz crystal microbalance sensor. The substrate chuck was rotated at 30 rpm during the deposition, in order to improve the uniformity of deposition.

Prior to coating with the WO_3|Pt dual coating, the n^+Si wafer pieces were etched in dilute hydrofluoric acid (HF) solution (50:1 H_2O:HF) to remove the surface oxide. HF is an extremely dangerous acid that should only be handled in a designated fume hood with proper chemically-resistant personal protective equipment and with a prior protocol established for disposal of HF waste.

Electrode Preparation

Photoelectrodes were assembled by first physically etching a small area of the semiconducting film with a razor blade to reveal the underlying metallic back contact and then affixing tinned copper insulated hookup wire (Belden 8502-009) using conductive carbon paste (DAG-T-502, Ted Pella). Once stable, this electrode array was sealed in acid-resistant epoxy (Loctite Hysol E-120HP) and allowed to cure overnight. HER catalyst analogue electrodes were prepared similarly, with one additional step prior to making wire contact: the back surface of the coated n^+Si wafer pieces were etched with a diamond scribe while introducing indium gallium eutectic as back contact. The active area of each sample was measured using photography and image analysis software (ImageJ); measured working electrode areas ranged from 0.25 to 0.8 cm^2.

(Photo)electrochemical Measurements

The photoelectrochemical (PEC) experiments were performed under continuous simulated 1 Sun AM1.5G illumination from a 150 W Xe arc lamp solar simulator from ABET (calibration procedure described below). The front of the photoelectrode was illuminated through a fused silica window while bathed in 0.5 M H_2SO_4 electrolyte in a custom-built PEC reactor. All measurements were conducted in three-electrode configuration with a mercury/mercury sulfate ($Hg/HgSO_4$) reference electrode and an iridium wire (Ir/IrO_x) counter electrode using a Bio-Logic VSP potentiostat. In order to saturate the electrolyte with hydrogen gas (H_2) while displacing dissolved oxygen gas, the electrolyte was purged with

H_2 introduced through a porous glass gas dispersion tube for at least five minutes prior to electrochemical measurements. The reference electrode was calibrated to the reversible hydrogen electrode (RHE) scale by measuring the redox potential for the H^+/H_2 couple at a platinum working electrode in H_2-saturated electrolyte. The LSV experiments were conducted with a scan rate of 10 mV s^{-1} and the CA experiments were conducted by holding the working electrode at constant potential with respect to the reference electrode. For the 'dark' HER catalysis electrode, the experiments were conducted in 0.1 M $HClO_4$ electrolyte and durability was measured via chronopotentiometry (CP), wherein a constant current density was passed (-10 mA cm^{-2}) over the course of the experiment and the applied potential require to achieve this electrocatalytic output was measured as a function of time. The potentials displayed in the dark catalysis results were corrected for the series resistance of the electrochemical setup by measuring this resistance with electrochemical impedance spectroscopy and then subtracting the product of the current (i) and this resistance (R) from the V *vs*. RHE potential (E).

Lamp Calibration

Using an Ocean Optics Jaz EL 200-XR1 spectrometer, the absolute irradiance output from the Xe lamp was measured as illuminated through the quartz window of the PEC cell, without solution. The irradiance incident at the detector surface was manipulated by controlling the working distance between the lamp and the detector surface. This irradiance was considered to be calibrated to AM1.5G when the areal flux of above-bandgap photons (those with photon energy exceeding the bandgap energy of the material) was equal to the areal flux of above-bandgap photons in the AM1.5G solar spectrum, calculated using NREL's SMARTS2 worksheet.[1-3] The photon areal flux is estimated to vary by up to 5% from sample to sample due to the imprecision of manually aligning the electrode at the same distance from the lamp as the detector. The thickness of water between the front window of the PEC cell and the surface of each sample was about 4 cm; we did not compensate the illumination intensity for any absorption through this water layer.

Photocurrent Onset Potential Determination

The photocurrent onset potential was determined by taking the linear extrapolation of the main photocurrent onset feature to the point of intersection with the $j = 0$ axis (Figure S1), as reported previously.[4]

Calculation of Hydrogen Production and Comparison to Degradation

Hydrogen production is the dominant contributor to the photocurrent generated over the course of the experiment. This H_2 generation is evidenced by the sustained bubble formation at the electrode surface and the substantial total charge passed, approx. 20 000 C cm^{-2} or 0.2 mol e^- cm^{-2}, over the course of durability testing. This amount of charge is six orders of magnitude greater than that which could come from photoelectrode corrosion. The photoelectrode predominantly consists of CGSe (with a density of 5 g/cm^3 and a molecular weight of 668 g/mol) having a thickness of 2.5 μm, equivalent to approximately $2x10^{-8}$ mol $CuGa_3Se_5$ cm^{-2}. If every cation in the material were completely reduced to the metal over the course of the experiment (10 mol e^- per mol CGSe), this reduction would account for only $2x10^{-7}$ mol e^- cm^{-2}. The equivalent volume of H_2 corresponding to the amount of passed charge was calculated by converting the moles of electrons passed to moles of H_2 hypothetically produced (n = 2 mol e^- / 1 mol H_2) and then applying the molar volume of an ideal gas at 1 atm (22.4 L/mol).

Results

GI-XRD of an ultrathin WO_3 film

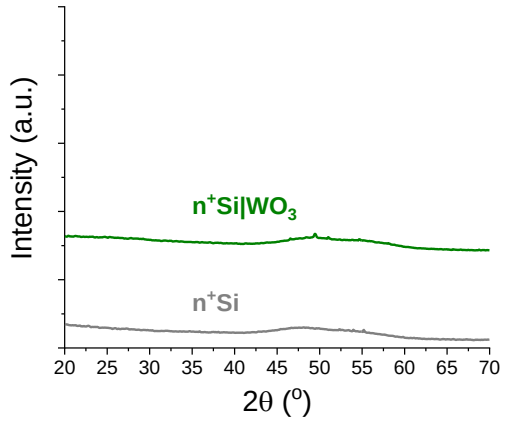

Figure S1: GI-XRD of an $n^+Si|WO_3$ sample (green) and a bare n^+Si wafer piece (gray) at an incidence angle of 1°; an offset in the data was imposed for clarity. The signals from the bare substrate and the coated sample are indistinguishable within the sensitivity of the measurement.

Cross-sectional SEM

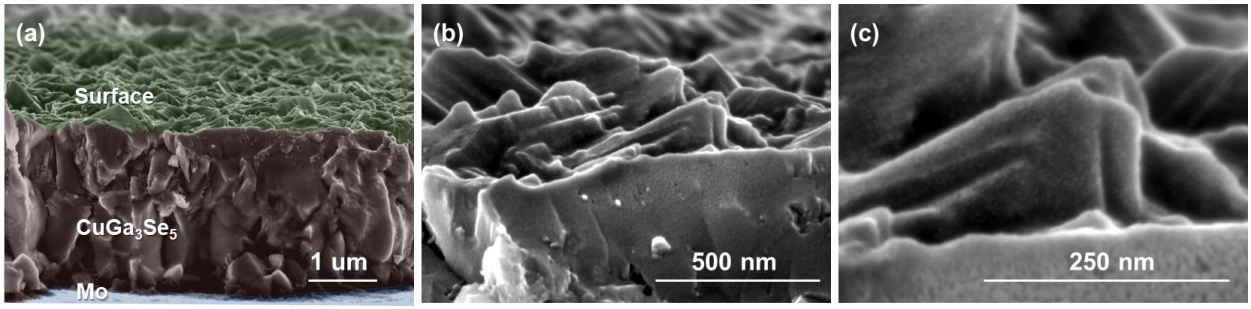

Figure S2: Cross-sectional SEM of an as-prepared $CuGa_3Se_5|WO_3|Pt$ device with the sample aligned at a shallow angle to capture more of the surface features (in the z-direction of the image) with false coloring and labels (a), a view focused on the apparent interface between the $CuGa_3Se$ and WO_3/Pt layers (b), and a view focused on a $CuGa_3Se_5$ crystallite with conformal coating of WO_3/Pt (from the 'Surface' region) (c).

UV/Vis Optical Characterization

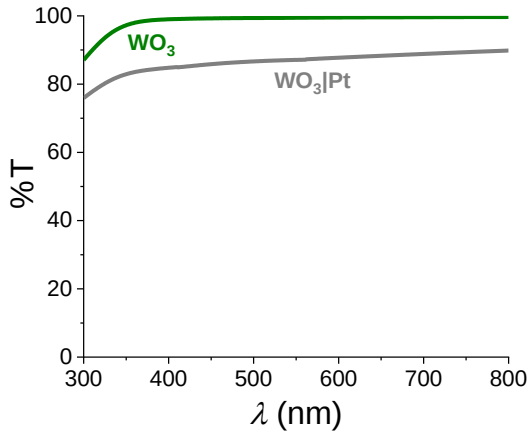

Figure S3: Transmittance measurements of an ultrathin WO_3 coating (green) and WO_3|Pt coatings (gray) on quartz substrates; measurements are baseline-corrected for the quartz substrate. It is apparent that the reflection/absorption of the Pt coating contributes much more substantially to lost photon flux than absorption by the WO_3 coating.

Photocurrent Onset Potential Determination

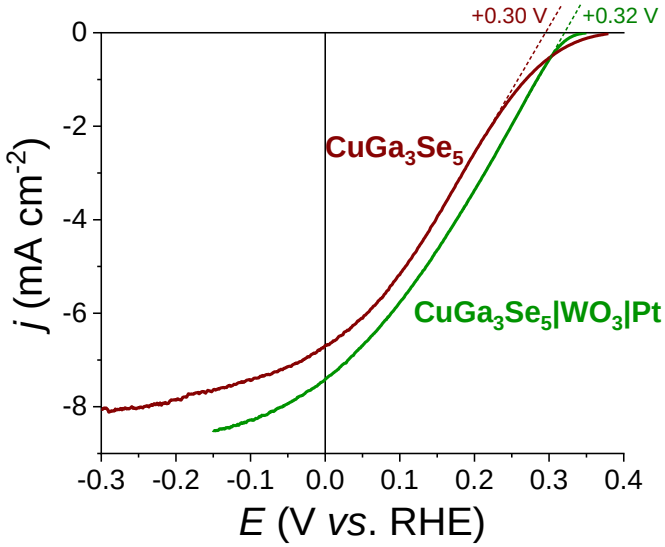

Figure S4: Photocurrent onset potential determination from the LSVs shown in Figure 2a, where the onset potential is defined as the intersection between the linear extrapolation of the main photocurrent onset feature and the $j = 0$ axis

PEC Activity with and without WO_3 coating

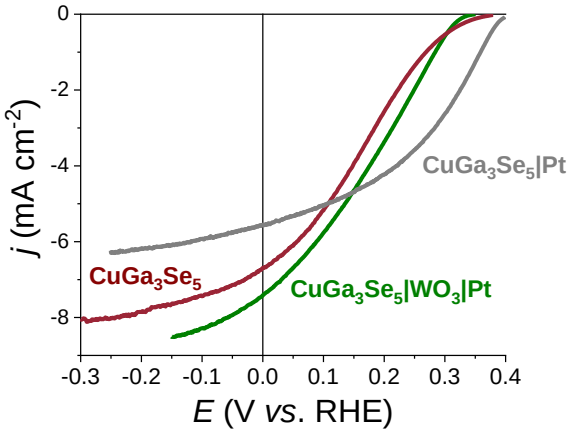

Figure S5: PEC LSV for three devices: $CuGa_3Se_5$, $CuGa_3Se_5$|Pt, $CuGa_3Se_5|WO_3$|Pt; all experiments were performed in 0.5 M H_2SO_4 electrolyte purged with H_2 gas, utilizing a $Hg/HgSO_4$ reference electrode and an Ir/IrO_x counter electrode under continuous simulated 1 Sun AM1.5G illumination. While the $CuGa_3Se_5$|Pt device demonstrates the expected onset potential improvement accompanying improved HER catalysis with Pt, the $CuGa_3Se_5|WO_3$|Pt apparently suffers from non-ideal behavior between the CuG_3Se_5 and the WO_3 coating so that there is minimal enhancement.

Idealized Band Diagrams

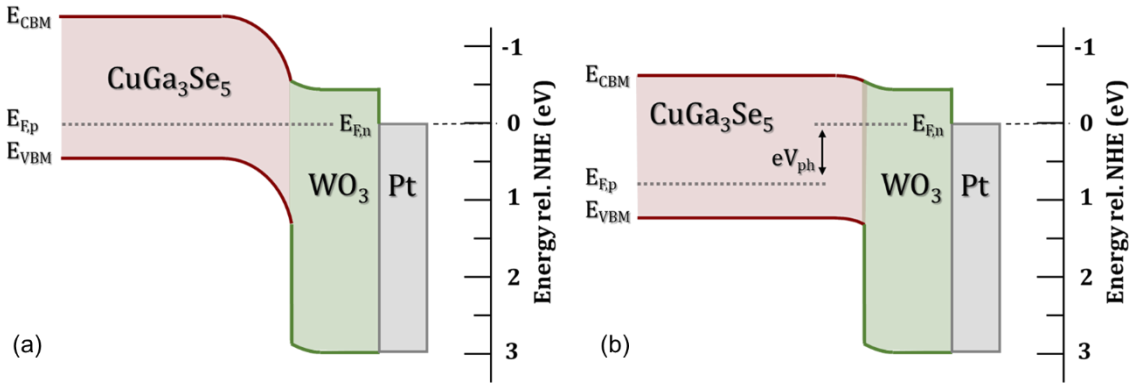

Figure S6: Idealized band diagram for a $CuGa_3Se_5|WO_3|Pt$ photocathode in equilibrium with acidic aqueous electrolyte (a) and under illumination in this same environment (b). $CuGa_3Se_5$ work function was determined by Kelvin probe measurements with a gold reference in air. The Fermi level ($E_{F,p}$) of $CuGa_3Se_5$ was determined as described below and the band gap of $CuGa_3Se_5$ is from Muzzillo, Klein, Li, DeAngelis, Horsley, Zhu, and Gaillard.[5] WO_3 data are from Bär, Weinhardt, Marsen, Cole, Gaillard, Miller, and Heske.[6] E_{CBM}, E_{VBM}, $E_{F,n}$, e, and V_{ph} refer to conduction band minimum energy, valence band maximum energy, Fermi level of the n-type WO_3, the charge of an electron, and photovoltage, respectively.

The Fermi level energy was determined by growing $CuGa_3Se_5$ on bare soda-lime glass. This sample was cleaved into a 1 cm^2 square and then soldered with indium onto the fours corners, upon which the room temperature Hall effect was measured, revealing a carrier concentration of 7.9e14 cm^{-3}. The $E_{F,n} - E_{VBM}$ value of 0.245 eV using the literature value for the effective hole mass of $CuGa_3Se_5$ ($0.56*m_0$) from Marín, Rincón, Wasim, Sanchez Pérez, and Molina Molina.[7]

PEC Durability with and without WO_3 coating

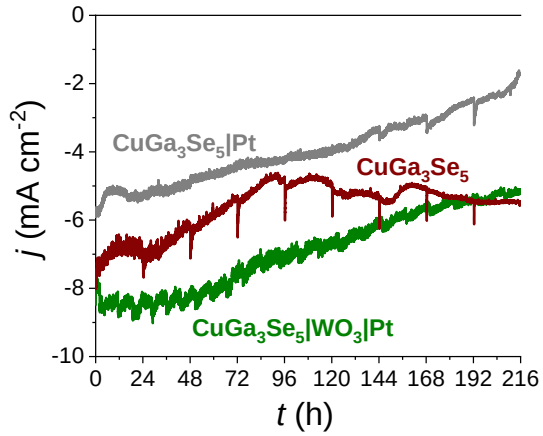

Figure S7: PEC CA for the three devices from Figure S4: $CuGa_3Se_5$, $CuGa_3Se_5|Pt$, $CuGa_3Se_5|WO_3|Pt$; all experiments were performed in 0.5 M H_2SO_4 electrolyte purged with H_2 gas, utilizing a $Hg/HgSO_4$

reference electrode and an Ir/IrO_x counter electrode under continuous simulated 1 Sun AM1.5G illumination

HER Catalysis

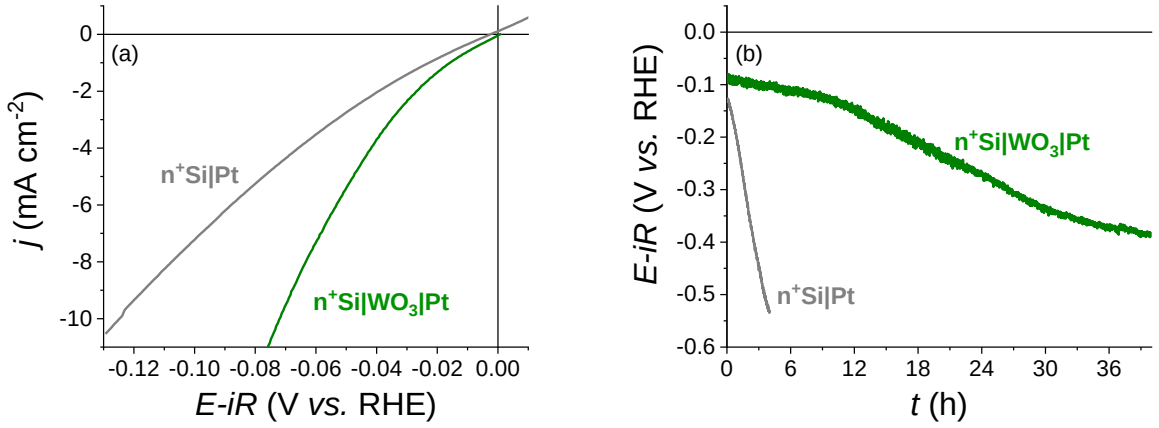

Figure S8: (a) LSV of an $n^+Si|WO_3|Pt$ electrode (green) and an $n^+Si|Pt$ electrode (gray) under 'dark' HER conditions and (b) CP of the same electrodes at -10 mA cm^{-2}; these experiments were conducted in 0.1 M $HClO_4$ electrolyte with $Hg/HgSO_4$ reference electrode, Ir/IrO_x counter electrode, and H_2 gas continuously bubbling through the electrolyte.

Long-term PEC Durability Testing

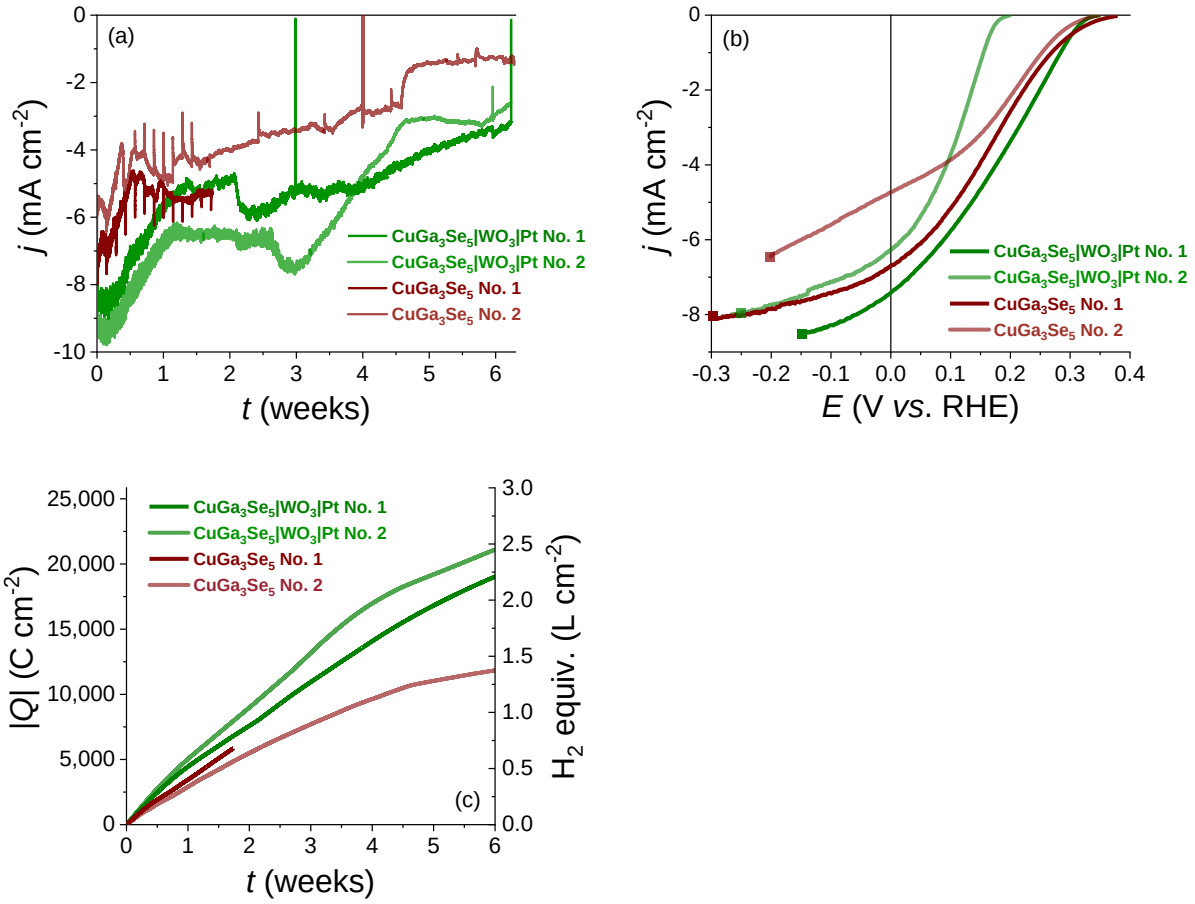

Figure S9: (a) PEC chronoamperometric durability testing for the four devices presented in Figure 2; the light was briefly blanked at several points throughout the experiments (at 3 weeks and 6 weeks for $CuGa_3Se_5|WO_3|Pt$ No. 1, at 4 weeks for $CuGa_3Se_5$ No. 2, and at 6 weeks for $CuGa_3Se_5|WO_3|Pt$ No. 2) to demonstrate that nearly all of the generated current is due to the light impetus; (b) PEC LSV for these same devices, with E_{CA} denoted with a square for each device, and (c) the charge passed as a function of time for these same devices; all experiments were performed in 0.5 M H_2SO_4 electrolyte purged with H_2 gas, utilizing a $Hg/HgSO_4$ reference electrode and an Ir/IrO_x counter electrode under continuous simulated 1 Sun AM1.5G illumination. The disparity in saturation photocurrent density has been previously noted in comparing samples from different batches when the absorber stoichiometry approaches the $CuGa_3Se_5$ employed in this study.[5]

SEM-EDX Analysis

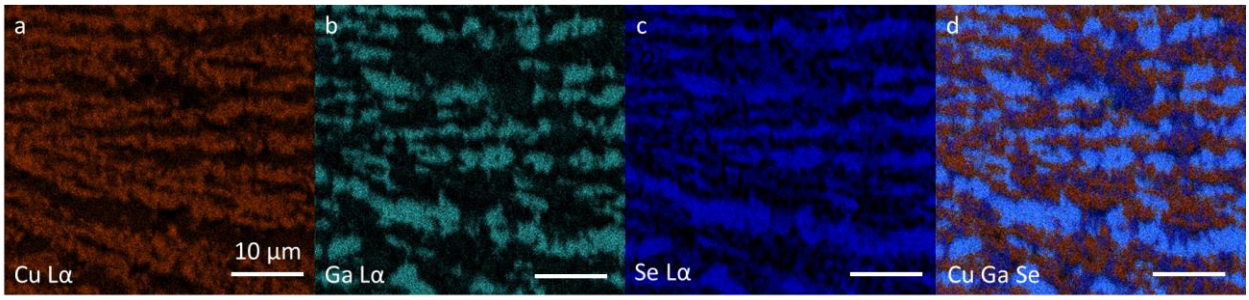

Figure S10: EDX elemental maps of the Cu Lα (a), Ga Lα (b), Se Lα (c), and the Cu, Ga, and Se composite (d) signals from a $CuGa_3Se_5|WO_3|Pt$ photocathode after six weeks of CA durability testing; all of the scale bars are 10 µm in length.

GI-XRD of $CuGa_3Se_5|WO_3|Pt$ devices

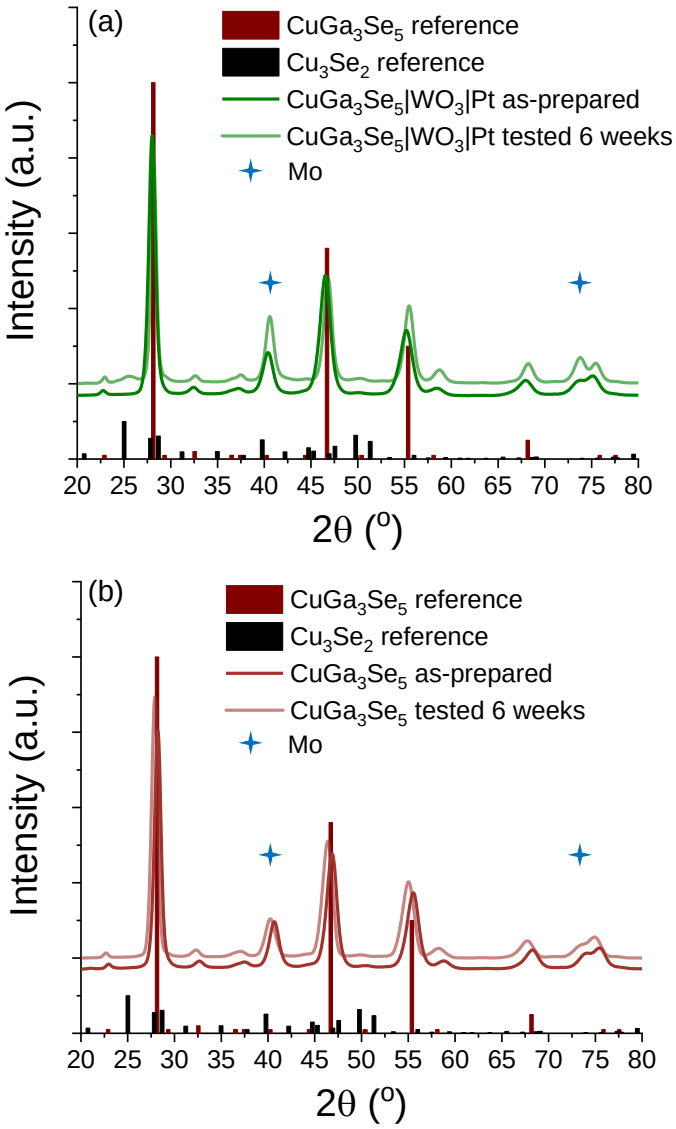

Figure S11: GI-XRD of $CuGa_3Se_5|WO_3|Pt$ devices (a) and $CuGa_3Se_5$ devices (b) before (dark colors) and after (pale colors) long-term operation, measured at an incidence angle of 5°; the diffraction patterns are well-matched to a $CuGa_3Se_5$ reference pattern (00-051-1223). The crystalline component of the $CuGa_3Se_5$ absorber layer remains largely unchanged before and after long-term operation, with the exception of a minor peak arising near $2\theta = 25°$ after testing in the $CuGa_3Se_5|WO_3|Pt$ case. A database search revealed Cu_3Se_2 (00-047-1745) to be the most plausible compound contributing its major diffraction peak near $2\theta = 25°$. The WO_3 and Pt layers appear to be undetectable under these measurement conditions, both before and after electrochemical testing. The two peaks arising from the Mo substrate are identified with blue diamond symbols.[5]

References

1. Gueymard, C. SMARTS: Simple Model of the Atmospheric Radiative Transfer of Sunshine https://www.nrel.gov/rredc/smarts/ (accessed Nov 3, 2019).
2. Gueymard, C. Parameterized Transmittance Model for Direct Beam and Circumsolar Spectral Irradiance. *Sol. Energy* **2001**, *71*, 325–346.
3. Gueymard, C. *SMARTS2, A Simple Model of the Atmospheric Radiative Transfer of Sunshine: Algorithms and Performance Assessment*; Cocoa, FL, 1995.
4. Hellstern, T. R., Palm, D. W., Carter, J., DeAngelis, A. D., Horsley, K., Weinhardt, L., Yang, W., Blum, M., Gaillard, N., Heske, C., Jaramillo, T. F. (2019). Molybdenum Disulfide Catalytic Coatings via Atomic Layer Deposition for Solar Hydrogen Production from Copper Gallium Diselenide Photocathodes. ACS Applied Energy Materials, 2(2), 1060–1066.
5. Muzzillo, C. P., Klein, W. E., Li, Z., DeAngelis, A. D., Horsley, K., Zhu, K., & Gaillard, N. (2018). Low-Cost, Efficient, and Durable H_2 Production by Photoelectrochemical Water Splitting with $CuGa_3Se_5$ Photocathodes. ACS Applied Materials & Interfaces, 10(23), 19573–19579.
6. Bär, M., Weinhardt, L., Marsen, B., Cole, B., Gaillard, N., Miller, E., & Heske, C. (2010). Mo incorporation in WO3 thin film photoanodes: Tailoring the electronic structure for photoelectrochemical hydrogen production. Applied Physics Letters, 96(3), 032107.
7. Marín, G., Rincón, C., Wasim, S. M., Sánchez Pérez, G., & Molina Molina, I. (1999). Temperature dependence of the fundamental absorption edge in CuGa3Se5. Journal of Alloys and Compounds, *283*(1–2), 1–4.